JOURNAL OF MATERIALS SCIENCE 16 (1981) 1273–1284

Deformation and cracking during high-temperature scratching of a glass

J. D. B. VELDKAMP*, N. HATTU
Philips Research Laboratories, Eindhoven, The Netherlands

During scratching of lead glass at elevated temperatures the scratch hardness, the types of crack that appear and the length of the cracks have been investigated. It was found that the hardness decreases with increasing temperature. The hardness increases with rising scratching speed, but the increase disappears gradually with rising temperature. It was also found that some types of crack disappear with increasing temperature, whereas other types of crack became more pronounced. Also a new type of a long lateral crack was found at elevated temperatures. The length of some types of crack showed an unexpected dependence on load. The average length of the cracks first increased with temperature but decreased sharply above a certain temperature. An attempt is made to explain the observed effects in the hardness with the aid of a deformation model proposed for metallic glass while using existing knowledge on the structure of the glass investigated and the known interaction of the glass surface with water. The crack phenomena are explained in terms of the the known enhanced slow crack growth at elevated temperatures, the relaxation taking place in the glass surface and the occurrence of viscous flow at the crack tip at an even higher temperature.

1. Introduction

Grinding can be regarded as a multi-point scratching operation [1]. It has been shown that the study of single scratches greatly contributes to a better understanding of grinding [1]. In the case of a scratch made on the surface of a brittle material two main phenomena can be observed: plastic grooving and brittle cracking [1]. The cracks appear when the load on the scratching point is higher than a specific value [1]. Both phenomena, grooving and cracking, can be expected to be temperature dependent, and hence the temperature generated during grinding will effect them. An aim of the present investigation was therefore to assess this effect to gain a better understanding of the grinding process. The investigation also contributed to the development of a new technique: hot turning of glass to obtain a transparent surface [2].

During the scratching of a brittle material, plasticity, which is absent in tension, is brought about by the high stresses which are present in this higly localized and (on average) compressive deformation. Scratching, therefore, enables the measurement of the yield stress (this property is directly related to the scratch hardness [3]) as a function of e.g. strain rate (the strain rate is proportional to the scratching speed) and temperature, which gives information about the deformation mechanisms in brittle materials. In the present investigation the scratching hardness is defined for a sharp square pyramid with a leading plane and is equal to the quotient of the normal load and the projection of the contact surface in the horizontal plane. In the case of crystalline materials the yield stress will generally decrease with increasing temperature and decreasing strain rate [4]. At room temperature an increase of scratch hardness with scratching speed is also found for glass [5].

In glass, four types of crack have been found during scratching: chips, median, lateral and sub-

*Present address: Product Division Glass, N.V. Philips Gloeilampenfabrieken, Eindhoven, The Netherlands.

0022–2461/81/051273–12$03.20/0

surface cracks [5]. The propagation speed of the median and lateral cracks is about equal to the scratching speed [6], so that the crack length and hence the stress intensity factor can be investigated as a function of crack speed [5]. At room temperature the relation between applied load and crack length in the case of median and lateral cracks can generally be described by [5]

$$F_n = AKr\,(r + \tfrac{1}{2}Bb)^{1/2} \quad (1)$$

where F_n is the applied load, K is the stress intensity factor, r is the distance between the crack tip and the centre line of the groove, which will subsequently be called the crack size, b is the groove width and A, B are constants dependent on crack type and geometry of the scratching point. In a simpler form one may write for a large crack size compared with groove width [7]

$$F_n = A'Kr\,(r)^{1/2}. \quad (2)$$

By introducing the scratch hardness, H_s, expressed by

$$H_s = \frac{4F_n}{b^2} \quad (3)$$

into Equation 1 the threshold load for crack propagation, F_{nmin} can be derived when r is taken to be equal to $\frac{1}{2}b$

$$F_{nmin} = L\frac{K^4}{H_s^3} \quad (4)$$

where L is a constant.

The same result but with another constant is obtained by substituting Equation 3 into Equation 1. Below F_{nmin} material is removed by plastic cutting and above F_{nmin} by brittle cracking as well [1, 5]. Because K and H are temperature dependent it may be expected that F_{nmin} is temperature dependent also. Similarly, so is the material removed during the abrasive process. It was found that lateral cracks in glass did not always obey Equations 1 or 2. The experimental verification of these expressions at elevated temperatures was also one of the aims of this investigation.

The number of lateral cracks at room temperature varies with scratching speed but also with load [5]. The same applies to the types of crack that develop [1, 5]. Not very much is known yet about the influence of temperature on the appearance of certain types of crack and on the crack length in glass and hence on grindability; so these influences were also investigated.

The high-temperature scratching apparatus and other experimental details are described in Section 2. The results of the experiments made to determine the effect of temperature, load and speed on hardness, types of crack that appear, number of cracks per unit length and the length of the lateral cracks are given in Sections 3.1, 3.2 and 3.3, respectively. These effects are discussed in the same sequence in Sections 4.1, 4.2 and 4.3. Conclusions are given in Section 5.

2. Experimental procedure

Our experiments were carried out using a modified version of an apparatus described elsewhere [1]. The present apparatus (Fig. 1) consists of a balance with a diamond (D) underneath the left-hand arm (L) and a sample-holder driven by a motor (M).

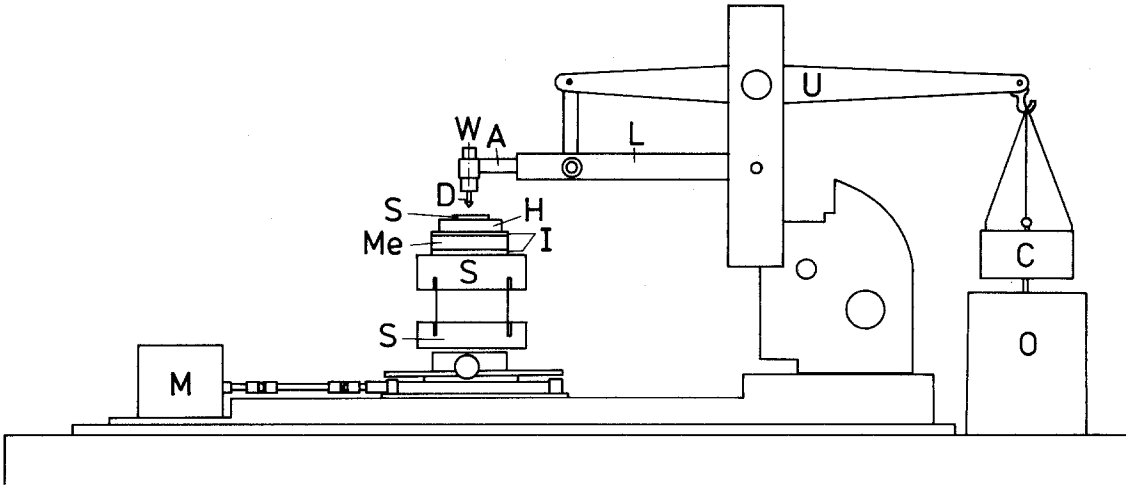

Figure 1 Longitudinal section of scratching apparatus for elevated temperatures.

The right-hand arm (U) is connected to a counterweight (C) and a damper (O). A load (W) can be placed on top of arm L above the diamond. Further details on the parts taken from the original apparatus can be found in [1]. The diamond holder is connected via an alumina shaft (A) to the left-hand arm in order to prevent warming up of the balance. The set-up underneath the diamond consists from top to bottom of the sample (S), a heating table (H), provided with a vacuum sample-holder, an insulating ceramic slab (I), a water-cooled metal slab (Me), another ceramic slab and a spring holder (S), in which the springs are provided with strain gauges. The spring-holder is mounted on a motor-driven carriage. The strain gauges are used to measure the tangential force. The elements* in the heating table are controlled by a power supply.† A standard sample measuring 40 mm x 20 mm x 5.5 mm was used. The temperature differences in such a sample while in contact with the diamond were measured on several materials by mounting thermocouples on the top and side faces of the sample. The maximum temperature difference on the top face was 40° C at a temperature in the centre of this face of 440° C. For the glass investigated, thermal stress can be expected to be low with respect to the stresses in the vicinity of the scratching point. The scratching temperature was taken to be equal to the temperature in the centre of the sample, which was the location of the scratches, the sample being calibrated for the temperature which was set by the controller.

Prior to an experiment the highly polished samples were annealed to remove residual stresses. In each experiment the sample was heated with the diamond resting on the surface, so that thermal equilibrium was easily obtained. Further details of the scratching experiments are given in [1]. In the experiments only a sharp square diamond pyramid with a semi-angle of 68° was used in the leading plane position. The tip radius was verified microscopically to be less than 0.5 μm. The loads used were between 0.1 and 1 N and the scratching speeds were between 10^{-7} and 10^{-3} m sec^{-1}. However, most of the experiments were carried out at 10^{-3} m sec^{-1}. The scratch length was about 10 mm. The scratch measurements were carried out after controlled cooling down to room temperature. The hardness was determined from the applied load and the groove width (see Section 1). To determine the hardness the groove width was measured from micrographs at about 10 locations. The distance between the centre line of the groove and the end of the crack was taken as the crack size. For the determination of the average size of one type of crack at least 20 crack sizes were measured. The sizes of the cracks were measured on micrographs with the aid of a digital length classifier.‡

The material investigated was SF 58§ glass. The composition of this glass was assessed by X-ray fluorescence analysis; the results are given in Table I.

3. Results

3.1. Hardness

Fig. 2 shows the scratch hardness of the glass as a function of load for three temperatures: 20, 160 and 365° C. The maximum, minimum and average hardness values are indicated. The hardness decreases with increasing load and with increasing temperature. The relative decrease in hardness within a load range of 0.3 to 1 N also diminishes with rising temperature.

Fig. 3 shows the hardness of the glass as a function of scratching speed, again for three temperatures: 20, 160 and 365° C. The relative increase in hardness within a speed range of 10^{-6} to 10^{-3} m sec^{-1} decreases with rising temperature. Fig. 4 gives the hardness as a function of temperature for a load of 0.5 N and a scratching speed of 10^{-3} m sec^{-1}. A gradual decrease is observed which becomes more pronounced above 450° C.

3.2. Types of crack, their fractions and numbers

The subsurface cracks gradually disappear with increasing temperature (see Fig. 5a and b). Both

TABLE I Composition in weight percentage of SF 58 glass

PbO	SiO_2	B_2O	Na_2O	Al_2O_3	K_2O	Sb_2O_3
76.1	21.3	1.33	0.54	0.10	0.68	0.03

*Standard cartridge heaters, Vulcan, USA.
†Getrosis, Philips, Holland.
‡MOP–Kontron Am 1, Kontron, Germany.
§Schott, Germany.

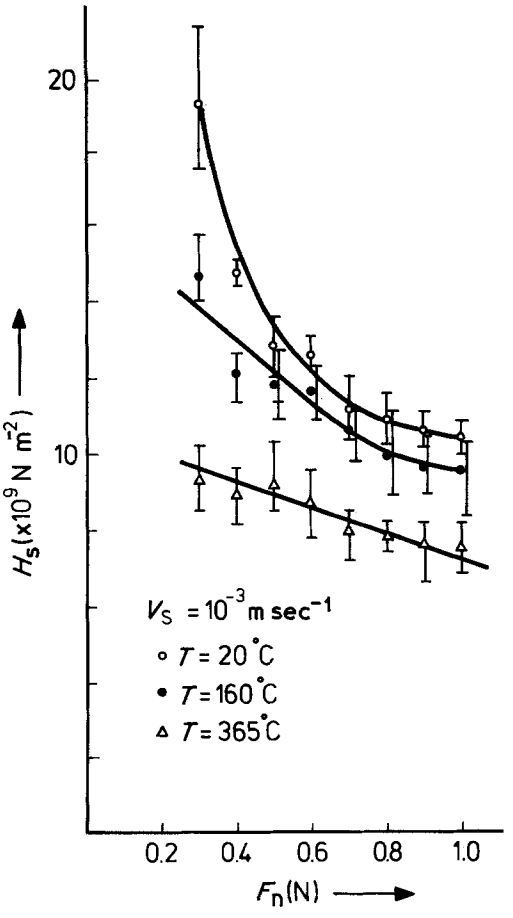

Figure 2 Scratch hardness as a function of normal load at three temperatures.

median and lateral cracks were found up to a specific temperature. In Fig. 6 the lateral cracks are divided into normal lateral cracks, with (Ia) and without (Ib) a curl, short lateral cracks (II) and very long lateral cracks (III). All these types of cracks started at a certain angle to the groove direction. Furthermore very long lateral cracks starting parallel to the groove direction (IV) and chips (V) were found. The fractions of the total number of lateral cracks of a particular type of lateral crack were determined. Because the fraction of a type of crack had to be determined from at least 20 cracks, the number of chips over the crack length investigated was too low for this purpose. The same applies to the lateral crack types III and IV, respectively. Because both types were very long cracks, it was decided to take the numbers of these cracks together, so that generally enough cracks were present. For the same reason cracks of type Ia were added to the cracks of type Ib. Figs 7 to 10 give the fraction of the lateral cracks I, II and III + IV as a function of load for the four applied temperatures (20, 160, 320 and 365° C). The bars indicating the fractions were determined by the number of cracks plus and minus the square root of the number. At room temperature the fraction of type II gradually decreased with increasing load whereas the fraction of type I markedly increased. At 160° C (Fig. 8) a decrease in the fraction of type II was only found at relatively low loads. At relatively high loads the fraction of type I decreased, whereas the fraction of types III and IV that developed was significant. At 320° C (Fig. 9) types III + IV were present as the main fraction, except at relatively low loads. All the fractions were independent of load except for the relatively low loads. At these loads the fraction of types I and II decreased whereas the fraction of types III + IV increased with increasing load. At 365° C (Fig. 10) types III + IV were about as important as types I and II. At relatively low loads the fractions of types I and II showed a slight decrease with increasing load whereas the fraction of types III + IV showed a weak increase.

It has already been shown that only at room temperature does the total number of lateral cracks per unit scratch length increase with increasing load up to about 0.5 N [5]. Above this load and also in the whole load range at elevated temperatures, the number of cracks was roughly independent of load.

Whereas a significant fraction of types I and II was present over the whole load-range for all the temperatures, a significant fraction of types III + IV over the whole load range was only present at the two highest temperatures.

3.3. Crack length

The average crack size with its standard deviation (obtained from 20 to 66 crack sizes) as a function of applied load is given on a double logarithmic scale for the several types of lateral crack in Figs 11 to 14 for 20, 160, 320 and 365° C, respectively. These figures also give the average lateral crack size as a function of applied load for all the lateral crack types together. The crack size increased with increasing load and temperature.

For a quantitative describtion of these results the dependence of crack size (r) on load (F_n) is given as (see Equation 2)

$$F_n = A_1 K r^n \qquad (5)$$

where A_1 and n are constants to be determined

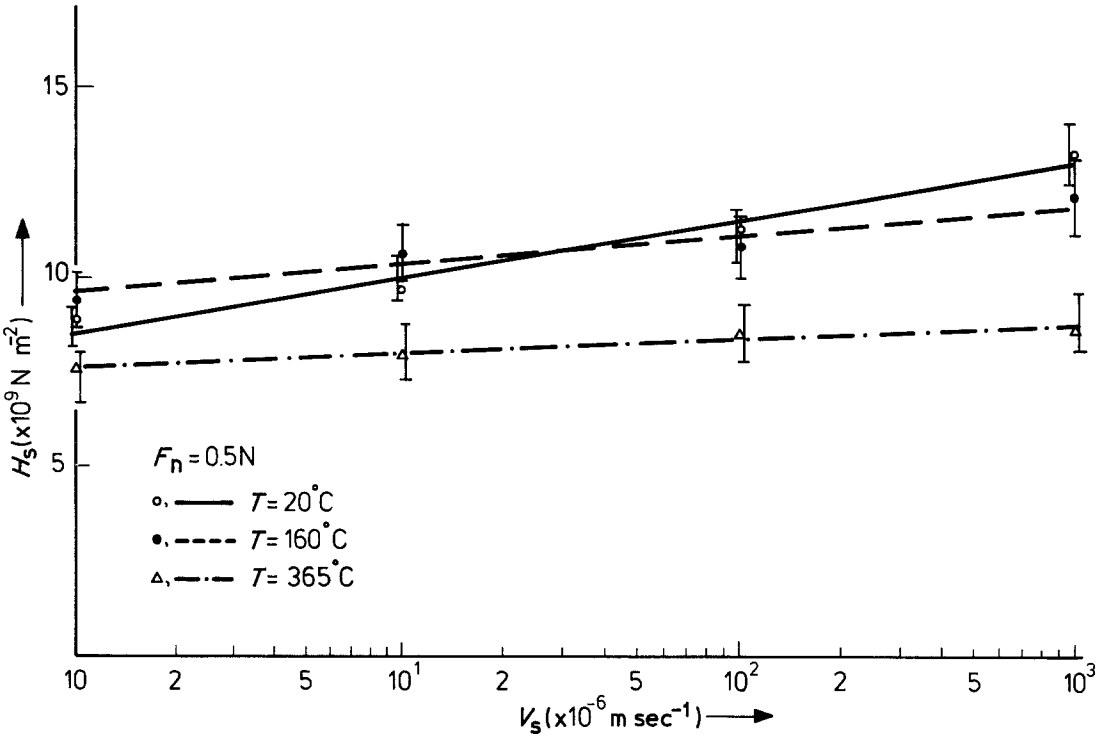

Figure 3 Scratch hardness as a function of speed for three temperatures.

from the plots. The n-values were obtained while omitting the measurements at the two highest loads, because in that part of the curves a clear plateau was present. For crack types III + IV no n-values according to Equation 4 were determined at 20 and 160° C, due to the low number of cracks present. The n-values are given in Table II. The tendency of the curves to follow the power $n = 1.5$ (see Equation 2) was present to some extent in the case of types I and II cracks at 20 and 320° C and for type II at 365° C. Very low n-values were found at 160° C. Other low n-values were found for types III + IV at 320° C and for type I at 365° C. A very high n-value was found for types III + IV at 365° C.

In Fig. 15 the crack size, averaged over the crack types at a load of 0.5 N and a scratching speed of 10^{-3} m sec^{-1}, is given as a function of temperature. The crack size increases with temperature, reaches a maximum and then decreases sharply.

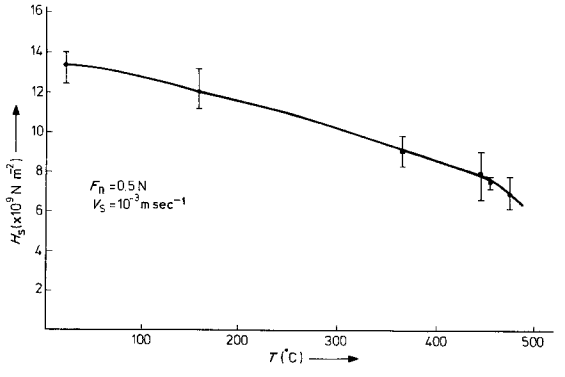

Figure 4 Scratch hardness as a function of temperature.

4. Discussion

4.1. Hardness

In this section first the relation between hardness, yield stress and Young's modulus is discussed, so that hardness effects can be directly related to yield stress effects. Moreover the proportional relationship between scratching speed and strain rate is elucidated. Then the observed phenomena in the hardness against load, hardness against strain rate and hardness against temperature plots are reduced to certain deformation regimes, which are explained by effects occurring in the structure of the glass.

The relationship between hardness (H), yield stress (Y) and Young's modulus (E) is, according to Johnson [3],

$$H = \tfrac{2}{3} Y \left(1 + \ln \frac{E \cot \theta}{3Y}\right) \qquad (6)$$

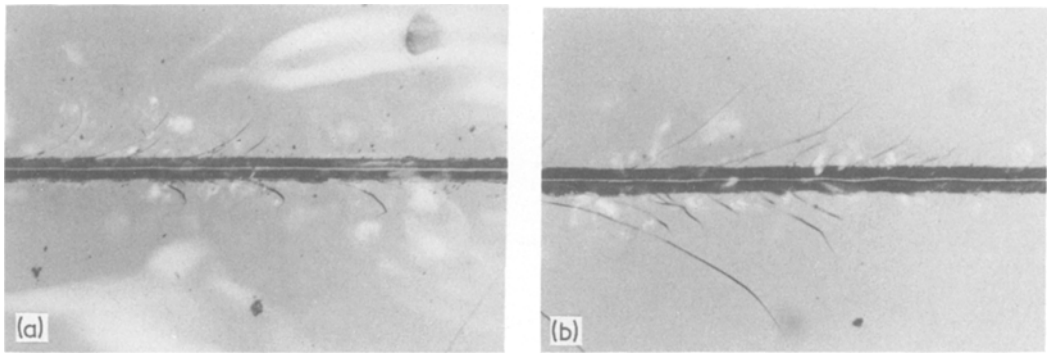

Figure 5 View from above of scratch at 20 and 320° C at a load of 0.5 N, (a) extended reflection spots due to subsurface crack at 20° C, or (b) disappeared at 320° C.

where θ is the semi-angle of the indenting square pyramid. E is only weakly dependent on temperature in the range investigated [8] and independent of strain rate. Thus strong influences of strain rate and temperature on the hardness must be due to influences on yield stress. From Equation 6 it is assumed that to a first approximation hardness is proportional to the yield stress.

During loading the hardness as measured from the size of the indentation or scratch in the contact region is independent of load [9, 10]. This means that the shape of the deformed volume of material is the same for any load. In the case of scratching this means that the average strain rate is proportional to the scratching speed and inversely proportional to the size of the deformed volume or to the width of the groove. Seen from the range of scratching speeds investigated, relatively small deviations can occur due to recovery of the groove during unloading. This will be the case in our experiments because the groove width and thus the size of the irrecoverable deformation was measured after the scratch experiments.

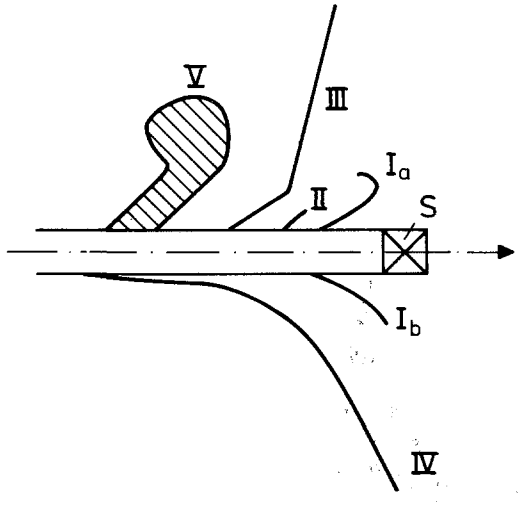

Figure 6 Schematic view from above of scratch with all the lateral crack types observed.

From Fig. 3 it can be concluded from the slope in the hardness against scratching speed plots, which diminishes with increasing temperature, that there is a strain rate and temperature dependent thermal part of the deformation. It will be shown later that the load dependency of the hardness (Fig. 2) is also due to this part of the deformation. From Fig. 4 in particular it can be seen that there also must exist a thermal part of the deformation which is only temperature dependent. Because the decrease of hardness with increasing temperature is less than that found for crystalline materials [11] it can moreover be concluded that there must exist in any case an athermal part of the deformation.

First a picture of the athermal part of the deformation is given. According to Yamane and Mackenzie [12] this deformation will be due to irrecoverable densification and to plastic flow. The contributions of the two types to the total irrecoverable deformation will depend on the type of glass [12, 13] and most likely on the temperature. The separate contributions are not determined for the lead glass investigated here. Both Yamane and Mackenzie [12] and Imaoka and Yasui [14] agree that the contribution of irrecoverable densification decreases as the number of network modifying ions is smaller. In the case of our glass (see Section 2) which probably consists of a mixture of a strong silicon oxide network and a weak lead oxide network [15], it can be expected that particularly plastic flow contributes to the deformation. However, Yamane and Mackenzie [12]

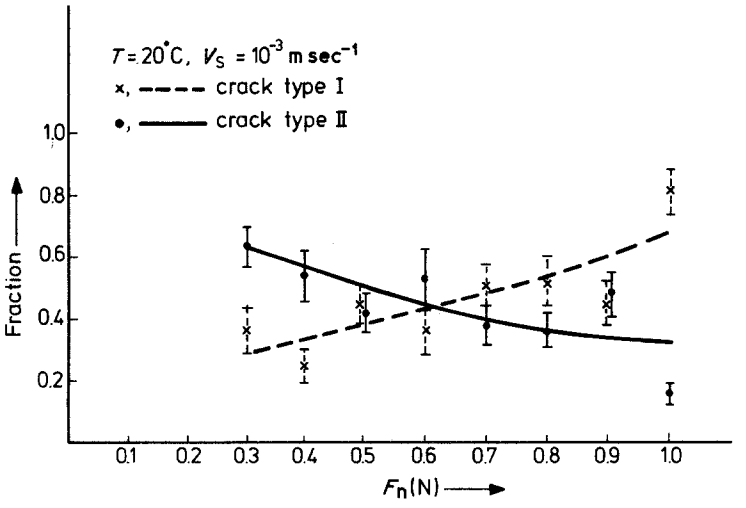

Figure 7 Fraction of crack types as a function of load at 20° C.

and Imaoka and Yasui [14] do not agree about the quantitative contributions.

According to Stevels [13] the irrecoverable densification is due to a structural change in the network produced by a change in co-ordination of the bridging ions. One can also imagine that the densification due to folding up of the network is partly irrecoverable due to the breaking of bridging bonds, in our case particularly bonds within the lead oxide network.

The plastic deformation of amorphous solids is generally observed to be strongly inhomogeneous [16]. One may also say that during deformation in the slip planes slipping areas are present amidst non-slipping areas. Formally the boundary between such a slipping area and the non-slipping surrounding material could be referred to as Somigliana dislocation [17], because length and direction of the slip vector's within the slipping area are not equal. When an amorphous solid is assumed to be formed by the introduction into a crystal of a network of very closely spaced dislocations, one can consider the plastic deformation as the movement of Somigliana dislocations through a dislocation network. The slip itself is suggested from microvoids which move due to a shear stress [16, 17]. In oxide glasses such voids or interstices are widely accepted for the description of the structure [13]. A temperature independent (or weakly dependent) movement of these voids can only be imagined when bridging bonds within the silicon oxide network are broken.

The temperature dependent thermal part of the deformation cannot be based upon a diffusion process. It is therefore likely that this part of the deformation is also related to the breaking of bonds. The temperature dependency of the bond strength of the bridging bonds within the lead

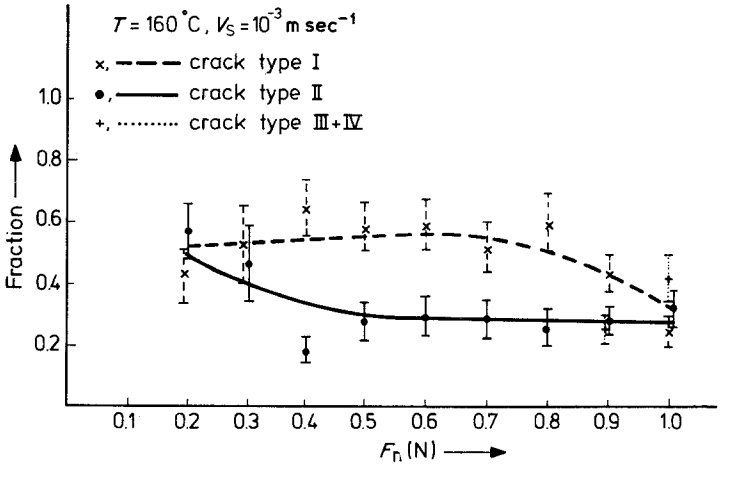

Figure 8 Fraction of crack types as a function of load at 160° C.

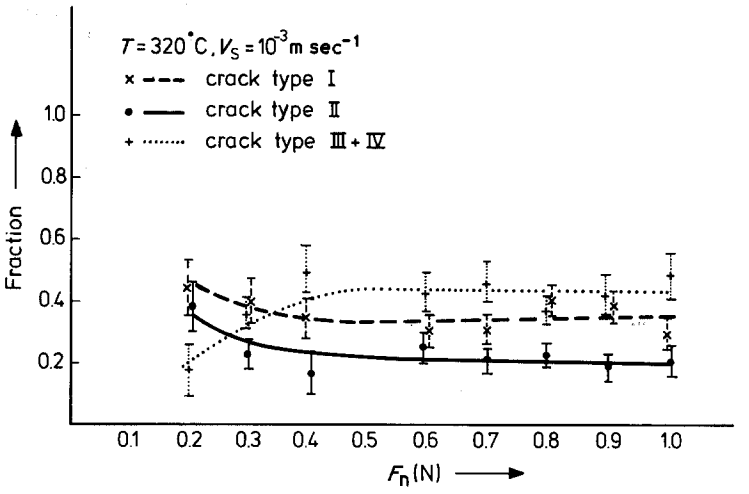

Figure 9 Fraction of crack types as a function of load at 320° C.

oxide network will be stronger than the temperature dependency of the bond strength of bridging bonds within the silicon oxide network. It can be imagined that when bonds within the lead oxide network are broken, the location of the bridging bonds within the silicon oxide network also changes which can lead to a reorientation of the interstices and so to a temperature dependent plastic deformation. This would imply that the temperature dependent thermal part of the deformation of a pure silica glass must be almost absent.

The temperature and strain rate (time) dependent thermal part of the deformation is due to an elastic recovery which is caused by the presence of water. Kranich and Scholze [10] showed that the dependency of indentation hardness of an oxidic glass on indentation time is due to the presence of water. Westbrook and Jorgensen [9] showed the same for oxidic crystalline materials. Moreover they showed that the time dependent part of the deformation disappears on increasing the temperature which agrees well with our observations. According to Westbrook and Jorgensen [9] increasing the temperature promotes desorption of water. The effect of the water might be diffusion of the water into the glass and the breaking of bridges in the network and hence oxygen ions being replaced by a double of much weaker OH ions [13].

The load dependency of the hardness is also due to the mechanism described above. It is clearly shown by Kranich and Scholze [10] that the size of the recovery after indentation is independent of load so that the relative increase of hardness due to recovery becomes smaller the higher the load. An explanation might be that diffusion of

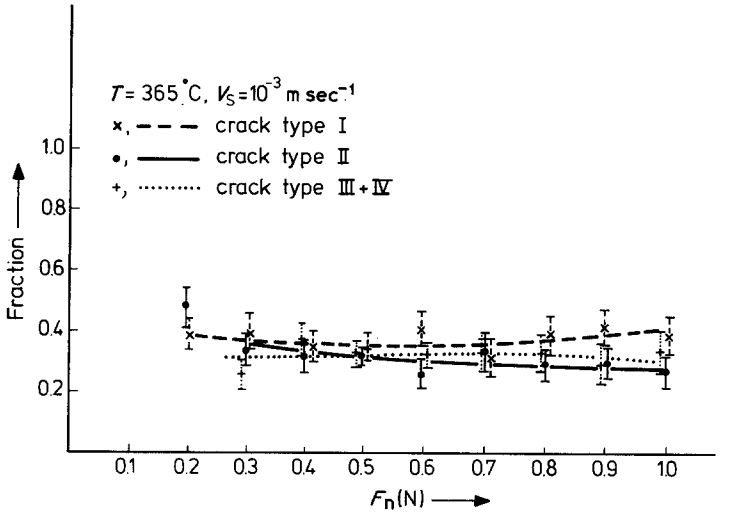

Figure 10 Fraction of crack types as a function of load at 365° C.

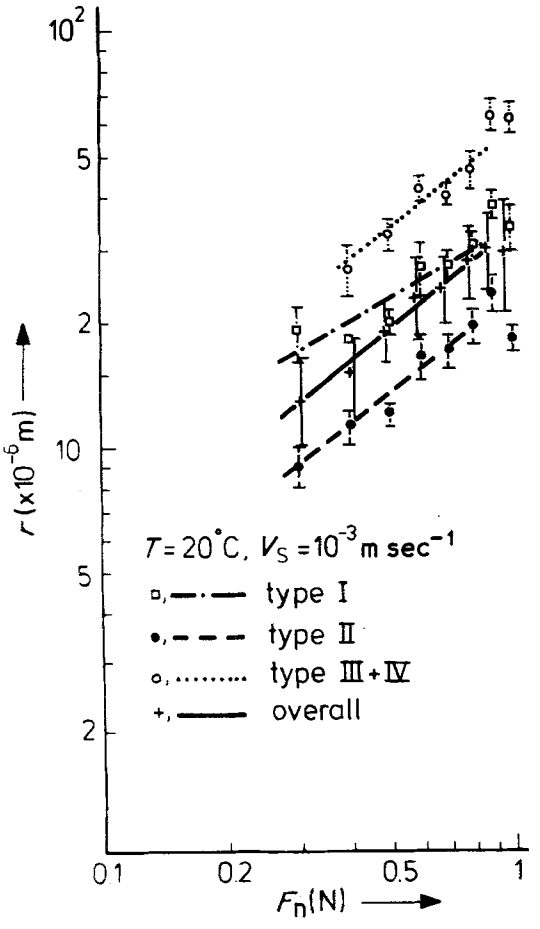

Figure 11 Crack size as a function of load for the different crack types and for all the crack types together at 20° C.

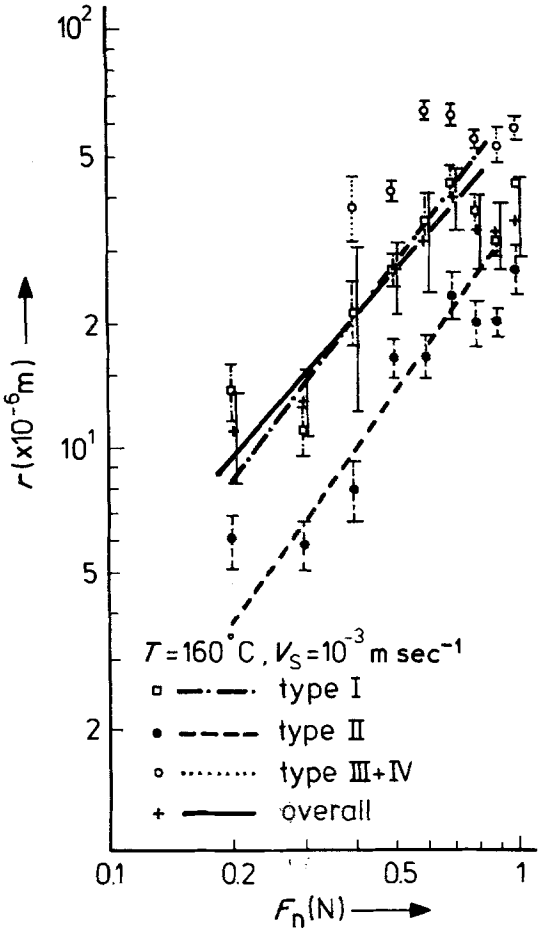

Figure 12 Crack size as a function of load for the different crack types and for all the crack types together at 160° C.

water into the glass might be governed by stress as in the case of Nabarro–Herring creep. So that it is not the load but the stress that determines the penetration depth of the water.

4.2. The types of crack, their fractions and numbers

It has already been discussed in Section 4.1 that due to the presence of water an inelastic recovery takes place after passing of the scratching point which disappears on increasing the temperature. This recovery leads to the development of the subsurface cracks. Not only the load dependency and the strain rate dependency of the hardness but also the subsurface cracks thus disappear on increasing the temperature.

The growth of cracks during scratching was filmed by Busch [6]. It can be observed in these films that the lateral cracks are generally initiated in front of the scratching point at a relatively high speed. When they do not grow out, one obtains crack type II. When they do grow out, they have a speed about equal to the scratching speed. When cracking stops, as a result of too great a distance between crack origin and scratching point, the cracks will show up as crack type I.

From Figs 7 to 10 and Section 3.2. one can conclude that on an average the fraction of type I decreases above 160° C and that the fraction of type II decreases above 20° C, while the average fraction of types III + IV increases. At 160° C the fraction of types III + IV apparently increases with increasing load at the cost of the fraction of type I. The fraction of types III + IV is fully present at 320 and 365° C. At low load and at 320° C the fraction of types III + IV increases with increasing load at the cost of types I and II. At 20° C the fraction of type I increases with increasing load at the cost of type II. Thus from this investigation one can also conclude that type

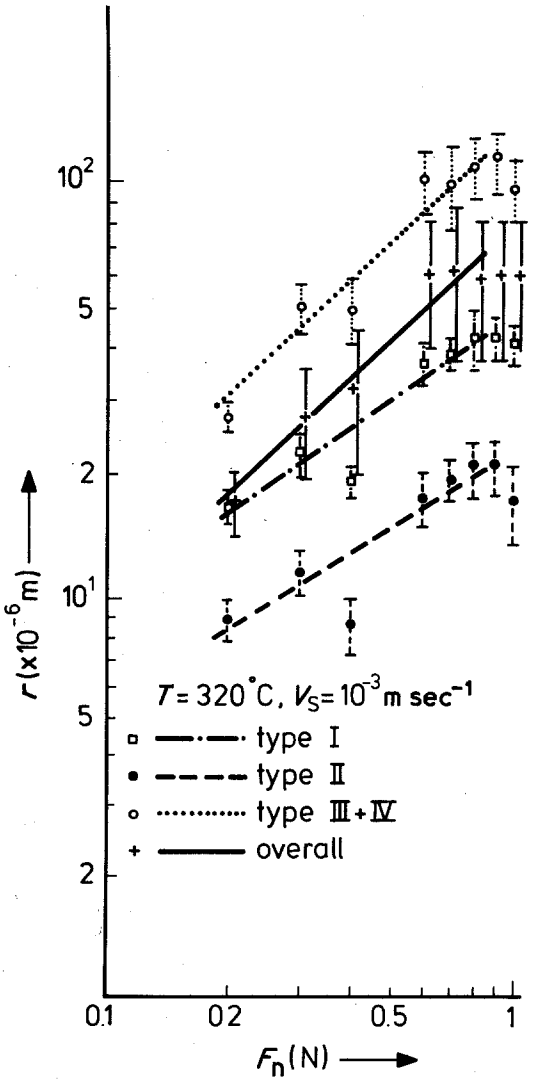

Figure 13 Crack size as a function of load for the different crack types and for all the crack types together at 320° C.

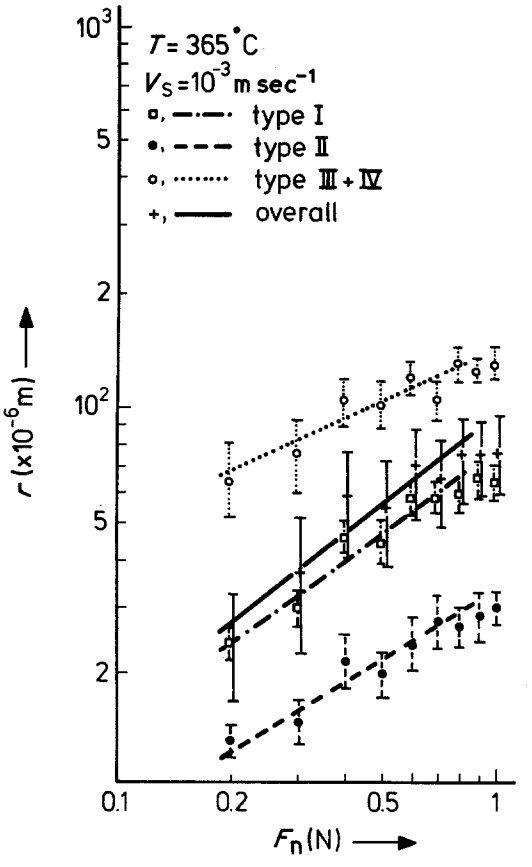

Figure 14 Crack size as a function of load for the different crack types and for all the crack types together at 365° C.

II is an initiation stage of type I; similarly types III + IV develop particularly from type I. As a matter of fact it can be deduced from the shape of the cracks that it must be type III that develops from type I. The appearance of crack types III + IV at elevated temperatures must be explained in terms of a larger crack speed at a particular K value (or a lower K at a particular crack speed) at these temperatures, so that a bigger crack size with respect to room temperature can develop.

There is no simple explanation for the initation of type IV. The further growth of this crack will be similar to crack type III.

It has already been observed at room temperature that above a specific load the number of cracks becomes independent of load [5]. Because slow crack growth is apparently more pronounced at elevated temperatures than at room temperature, it might be that the specific load (Equation 3) is lowered with respect to the room temperature value so that the number of cracks is independent of load.

4.3. Crack length

In this section first the plateau observed for all the crack types in the r–F_n plots (see Section 3.3 and Figs 11 to 14) will be discussed. The different dependency of the overall average size of the

TABLE II Value of n from Euqation 5 for different types of crack at different temperatures

Crack type	20° C	160° C	320° C	365° C
Type I	1.74	0.76	1.52	1.15
Type II	1.29	0.72	1.68	1.56
Type III + IV	—	—	1.09	2.28
Average	1.27	0.89	1.10	2.33

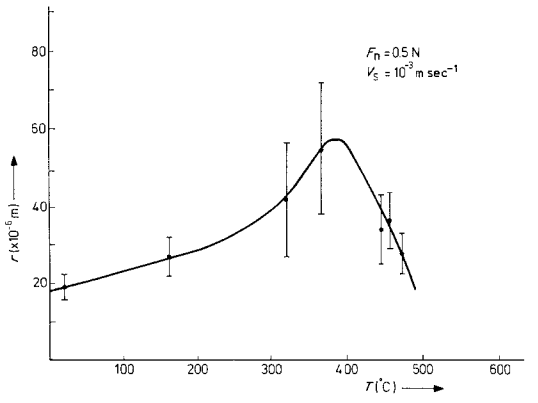

Figure 15 Crack size of all the crack types together as a function of temperature.

lateral cracks on load, as expressed in the value of n (see Section 3.3) is discussed for the four temperatures investigated. The load ranges taken into account are rather low so that only pronounced differences in n-values will be discussed. Then the n-values of the separate crack types at one temperature will be compared and furthermore the n-values of each crack type at the different temperatures will be compared. Finally, the dependency of the overall average size of the lateral cracks on temperature at one load will be discussed.

When there is a direct contact between indenter and crack origin, it can be expected, that for the case when only median and lateral cracks are present, Equations 1 or 2 are approximately valid. However, in reality an increasing distance in the scratch direction between crack origin and indenter is observed, which means that the power n in Equation 5 becomes much higher than 1.5. This is observed as a plateau in the r–F_n plot.

Particularly striking is the low n-value of the overall average crack size at 160° C. Such an increased dependency of crack size on load can only be related to an increased influence of water. However, the influence of water on hardness (Section 4.1) is already diminished at 160° C. A tentative explanation for this contradiction might be that the formation of new crack surface attracts water which promotes desorption of the original glass surface. This promotion of desorption together with the water from the air gives an increased water transport to the crack tip and so an enhanced crack growth.

The relatively high n-value for type I at 20° C might be related to the simultaneous growth of median, lateral and subsurface cracks at this temperature. The very low value of n for type III + IV at 320° C can be explained by a relatively high sensitivity for water of this type of crack at this temperature. The relatively low final speed of crack type III + IV apparently enables the onset of viscous flow at the crack tip at 365° C leading to a very high n-value in that case. For this reason it is interesting to see that crack type I with a relatively higher crack tip speed has a relatively low n-value at 365° C. At this speed viscous flow is apparently not possible at the crack tip.

For the reasons mentioned above the initial increase of crack length with temperature (Fig. 15) is explained by an enhanced stress corrosion due to water with increasing temperature. The transition to a decrease in crack length with increasing temperature will be due to viscous deformation at the crack tip.

5. Conclusions

(1) The length of the lateral cracks produced during the scratching of the glass initially increases with increasing temperature due to enhanced stress corrosion. However, probably due to viscous deformation at the cracktip the entire cracking disappears above a certain temperature, which enables crack free grinding or turning.

(2) The volume of material per unit energy removed by grinding will roughly increase with increasing temperature at first. But above a certain temperature a decrease starts which results in a volume per unit energy much lower than at room temperature.

(3) The grooving deformation obtained during scratching of the glass is suggested to be divided into an athermal part particularly due to plastic deformation, a temperature and strain rate dependent thermal part due to water induced stress relaxation and a thermal part, which is only temperature dependent, due to breaking of bridging bonds in the PbO network of the glass investigated and to reorientation of the interstices. At elevated temperatures the glass behaves almost as an ideal plastic material during scratching.

(4) The dependence of hardness on scratching speed, which is already low at room temperature compared to crystalline materials, decreases with increasing temperature. The dependence of hardness on load also disappears with increasing temperature. Both effects are suggested to be due to a water induced stress relaxation effect.

(5) Subsurface cracks disappear with increasing temperature roughly simultaneously with the load and strain rate dependency of the hardness. Therefore they are probably also due to the water induced stress relaxation.

(6) Apart from "normal" lateral, median and subsurface cracks, very long lateral cracks were found at elevated temperatures in two crack types; one of a normal shape and one which is initiated almost parallel to the scratching direction.

(7) Probably due to the occurence of different crack and deformation effects at different temperatures there are no simple and unequivocal relations between applied load, stress intensity factor and crack length.

Acknowledgement

The authors wish to thank Dr A. Broese van Groenou, Dr G. de With, Mr H. Verwey and Mr P. T. Logtenberg for many discussions and helpful suggestions. They are indebted to Mrs E. W. J. M. van Meijl and H. J. M. Hermans for the analysis of the SF 58 glass, and to Mr W. G. M. Kempen for making the statistical programs.

References

1. A. BROESE VAN GROENOU and J. D. B. VELDKAMP, *Philips Tech. Rev.* **38** (1978/79) 69.
2. R. BREHM, K. VAN DUN, J. C. G. TEUNISSEN and J. HAISMA, *Prec. Eng.* **1** (1979) 207.
3. K. L. JOHNSON, *J. Mech. Phys. Sol.* **18** (1970) 115.
4. R. W. K. HONEYCOMBE, "The Plastic Deformation of Metals", (Arnold, London, 1974).
5. J. D. B. VELDKAMP, N. HATTU and V. A. C. SNIJDERS, in "Fracture Mechanics of Ceramics 3", edited by R. C. Bradt, D. P. H. Hasselman and F. F. Lange, (Plenum, New York, 1978).
6. D. M. BUSCH, Films E1328–E1330, Inst. Wiss. Film. Göttingen, 1967.
7. B. R. LAWN and E. R. FULLER, *J. Mater. Sci.* **10** (1975) 2016.
8. V. I. PRIMENKO, A. N. SHIRYAEVA and V. I. GALYANT, *Glass Ceram.* **35** (1978) 666.
9. J. H. WESTBROOK and P. J. JORGENSON, *Trans. Met. Soc. AIME* **233** (1965) 425.
10. J. F. KRANICH and H. SCHOLZE, *Glastechn. Ber.* **49** (1976) 135.
11. T. N. LOLADZE, G. V. BOKUCHAVA and G. E. DAVIDOVA, in "The Science of Hardness Testing and its Applications", edited by J. H. Westbrook and H. Conrad (American Society for Metals, Metals Park, Ohio, 1973).
12. M. YAMANE and J. C. MACKENZIE, *J. Non-Cryst. Sol.* **15** (1974) 153.
13. J. M. STEVELS, in "Handbuch der physik XIII", edited by S. Flügge (Springer, Berlin, 1962).
14. M. IMAOKA and I. YASUI, *J. Non-Cryst. Sol.* **22** (1976) 315.
15. E. M. RABINOVICH, *J. Mater. Sci.* **11** (1976) 925.
16. C. A. PAMPILLO, *ibid.* **10** (1975) 1194.
17. J. C. M. LI, in "Frontiers in Materials Science", edited by L. E. Murr and C. Stein (Marcel Dekker, New York, 1976).
18. R. J. CHARLES, in "Fracture Mechanics of Ceramics 4", edited by R. C. Bradt, DPH Hasselman and F. F. Lange (Plenum, New York, 1978).

Received 1 September and accepted 22 October 1980.